

# The inactive form of recA protein: the 'compact' structure

Rob W.H. Ruigrok<sup>1</sup>, Bernd Bohrmann<sup>2</sup>,  
Elizabeth Hewat<sup>3</sup>, Andreas Engel<sup>4</sup>,  
Eduard Kellenberger<sup>2</sup> and Elisabeth DiCapua<sup>1</sup>

<sup>1</sup>European Molecular Biology Laboratory, Grenoble Outstation, BP 156, F-38042 Grenoble Cedex 9, France, <sup>2</sup>Abteilung für Mikrobiologie, Biozentrum, Klingelbergstrasse 70, CH-4056 Basel, Switzerland, <sup>3</sup>Laboratoire de Biologie Structurale, CEA and CNRS URA 1333, DBMS/DSV, CENG, BP 85, F-38041 Grenoble Cedex, France and <sup>4</sup>Maurice E. Müller-Institut, Klingelbergstrasse 70, CH-4056 Basel, Switzerland

Communicated by E. Kellenberger

When recA protein is enzymatically inactive *in vitro*, it adopts a more compact helical polymer form than that of the active protein polymerized onto DNA in the presence of ATP. Here we describe some aspects of this structure. By cryo-electron microscopy, a pitch of 76 Å is found for both the self-polymer and the inactive complex with ssDNA. A smaller pitch of 64 Å is observed in conventional electron micrographs. The contour length of complexes with ssDNA was used to estimate the binding stoichiometry in the compact complex,  $6 \pm 1$  nt/recA. In addition, the compact structure was observed *in vivo* in *Escherichia coli*: inclusion bodies produced upon induction of recA expression in an overproducing strain have a fibrous morphology with the structural parameters of the compact polymer.

**Key words:** recA–DNA stoichiometry/recA helical parameters/recA storage form

## Introduction

recA protein of *Escherichia coli* is responsible for homologous recombination (via its strand exchange activity, reviewed in Roca and Cox, 1990; Kowalczykowski, 1991) and for the control of the SOS system of DNA repair [via cleavage of LexA protein, the repressor of the genes coding for this system (Little and Mount, 1982; Silatly and Little, 1987)]. *In vitro*, these activities of the protein depend on the presence of ATP (or its non-hydrolysable analogue, ATP $\gamma$ S), and DNA. The active ternary complexes have been studied extensively by electron microscopy (EM) and by solution scattering: recA forms filamentous complexes with the DNA, in which 3 bp of dsDNA or 3–6 nucleotides per protein unit (the stoichiometry for ssDNA is still a matter of dispute) are bound inside a helical sheath of six recA units per turn of 95–100 Å pitch (DiCapua *et al.*, 1982; Egelman and Stasiak, 1986).

Under conditions where no enzymatic activities are observed, i.e. in the absence of nucleotide cofactor or DNA or both, recA also polymerizes into a filamentous structure (Koller *et al.*, 1983; Williams and Spengler, 1986) which by EM appears more compact, reflecting a helical arrange-

ment of recA with a smaller pitch. This arrangement has been described for recA self-polymers and self-polymers in the presence of ATP $\gamma$ S, as well as for the complex with ssDNA when no nucleotide is added (DiCapua *et al.*, 1990). The helical pitch value reported in the literature has varied considerably (Flory *et al.*, 1984; Stasiak and Egelman, 1986; Williams and Spengler, 1986; Heuser and Griffith, 1989). The value of 64 Å (Stasiak and Egelman, 1986) was lower than the value derived from neutron scattering in solution. It has therefore been suggested that classical EM specimen preparation leads to a reproducible shrinkage of the compact structure, which in solution has a pitch of 70–75 Å [DiCapua *et al.*, 1990; 75 Å was also observed by EM in amorphous ice for the pitch of the ssDNA complex by Chang *et al.* (1988)]. recA has crystallized in a helical self-polymer form (McKay *et al.*, 1980; Story *et al.*, 1992); the helix in the crystal has a pitch of 82 Å, with six recA units per turn.

In the present paper we discuss several aspects of the compact structure: the helical pitch, the binding stoichiometry with ssDNA and the mass per length; in addition, the compact conformation of the recA polymer is shown to be present *in vivo*, in inclusion bodies of recA overproducing bacteria.

## Results and discussion

### The pitch of the compact form

We have defined the 'compact form' as the filaments recA forms by self-polymerization or by binding to ssDNA in the absence of nucleotide cofactor, i.e. under circumstances when it does not form the enzymatically active, 'open' helical filaments (DiCapua *et al.*, 1990). Several approaches have been used to visualize the helical pitch of this structure; the values discussed in this paper are summarized in Table I; a synoptic table of the values from the literature can be found in Yu and Egelman (1992).

Cryo-electron microscopy (cryo-EM) was used to image recA self-polymers and recA complexes with ssDNA in amorphous ice. The filamentous structures as shown in Figure 1 were observed; their helical pitch was determined by measuring the length of stretches of 10 turns on a digitizer: both structures yielded values of 76 Å [Table II; for completeness, Table II also shows the pitch of the self-polymer in the presence of ATP $\gamma$ S (DiCapua *et al.*, 1992)]. The same pitch of 76 Å for complexes with ssDNA was found after incubation at room temperature or 37°C, even though the contour length was shorter after incubation at lower temperature (Materials and methods). A pitch of  $75 \pm 2$  Å was observed by Chang *et al.* (1988), and  $76 \pm 2$  by Yu and Egelman (1992), by cryo-EM for the compact complex with ssDNA.

The width of the self-polymers, measured from prints, was found to be  $106 \pm 7$  Å ( $n = 26$ ) and that of the ssDNA complexes was found to be  $110 \pm 7$  Å ( $n = 18$ ), in agreement with the 110 Å outer diameter of the model for

**Table I.** Summary of the pitches for the recA filaments discussed in this paper

Method	Pitch in Å ( <i>n</i> )
<i>Compact filament</i>	
EM negative staining after glutaraldehyde fixation	64 ± 2 (36)
EM negative staining without fixation <sup>b</sup>	short circles 59–63 <sup>a</sup>
	long circles 75 ± 4 (50)
EM in amorphous ice unfixed	76 ± 2 (38)
Small angle neutron scattering <sup>b</sup>	70 ± 5
EM of thin sections	76 ± 2 (16)
<i>Crystal structure<sup>c</sup></i>	
Open complex with DNA and ATP <sub>γ</sub> S	82.3 Å
By cryo EM <sup>d</sup> ds DNA	95 ± 2 (29)
	ssDNA 100 ± 2 (170)
By negative stain EM, fixed or unfixed <sup>d</sup>	dsDNA 94 ± 2 (30)
	ssDNA 96 ± 4 (30)
By small angle neutron scattering	95 ± 5

<sup>a</sup>This value is variable. The results of four independent experiments were: 63 ± 1 Å (*n* = 9); 63 ± 1 Å (*n* = 12); 59 ± 2 Å (*n* = 16); 63 ± 8 Å (*n* = 23).

<sup>b</sup>DiCapua *et al.*, 1990; <sup>c</sup>Story *et al.*, 1992; <sup>d</sup>Hewat *et al.*, 1991.

the compact complex from Fourier analysis of micrographs of samples in amorphous ice (Yu and Egelman, 1992).

In conventional EM specimens (fixed with glutaraldehyde, adsorbed to carbon films and stained with uranyl acetate), the self-polymers have a pitch of 63 Å (width 113 ± 10 Å, *n* = 41) and the compact ssDNA complexes, a pitch of 64 Å (width 121 ± 6 Å, *n* = 21) (Table II). By cryo-EM of unfixed samples, we only observed the 76 Å repeat, although the same sample solution prepared for negative stain EM in parallel clearly showed the 64 Å repeat.

### The stoichiometry of binding to ssDNA in the compact form

The stoichiometry of binding to ssDNA is of primary importance in all models of the molecular mechanism of the activity of the recA protein complex; this, however, concerns the complex in the presence of ATP (ATP<sub>γ</sub>S) and is not the subject of the present report. We are concerned here with the stoichiometry of binding in the absence of nucleotide cofactor. This value has been determined previously by protection from DNase as being 3 nt/recA (Bryant *et al.*, 1985). The binding to etheno-derivatized ssDNA can be monitored by the increase of fluorescence of the bound etheno-DNA; in this case, a titration point is observed at 3–8 nt/recA [3.5 in Menetski and Kowalczykowski (1985); 3.5 in Takahashi *et al.* (1989); 6 in Silver and Fersht (1982) and 8 in Cazenave *et al.* (1983)].

Here we used a different approach, namely measuring the contour length of complexes with circular ssDNA on electron micrographs at varying input stoichiometries, to determine this binding stoichiometry. We obtain the value from three points of view: (i) the saturation point in a titration curve; (ii) the shape of the titration curve; and (iii) the comparison of the derived mass per length (calculated from the axial rise per nucleotide of the saturated complex and the binding stoichiometry determined from the binding curve) with the mass per length obtained independently by neutron scattering and by scanning transmission EM (STEM).

This approach is valid under conditions of 'stoichiometric' binding of the recA to the DNA, i.e. under conditions optimized for full binding. Concentration of reactants (25 μM

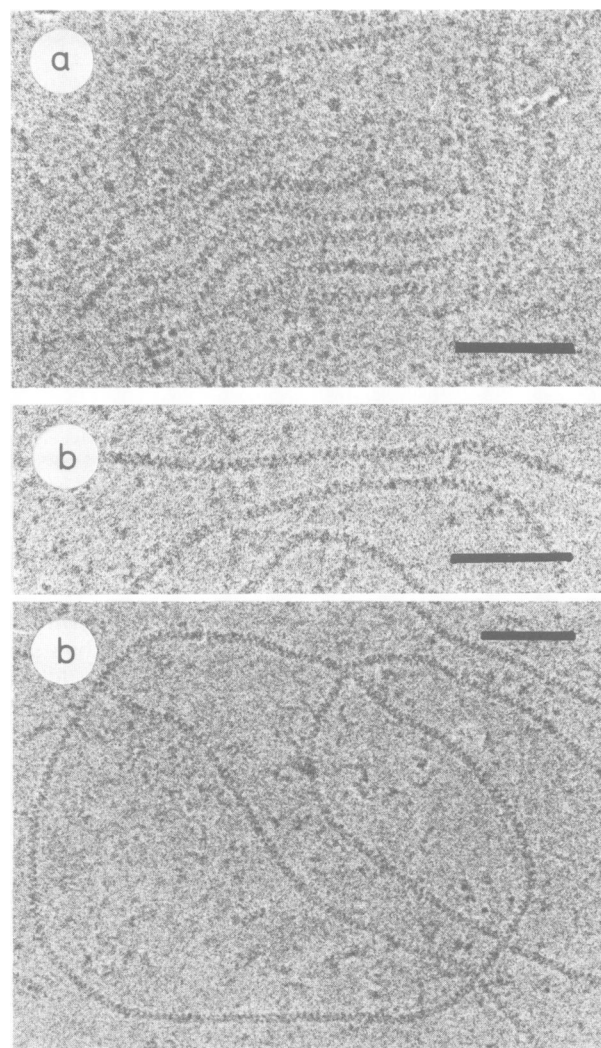


**Fig. 1.** RecA filaments in the compact form by cryo-electron microscopy. (a) Self-polymer; (b) Complex of recA with 6 nt/recA of ssDNA. Samples were 100 μM recA in 20 mM potassium phosphate and 2 mM Mg(acetate)<sub>2</sub>. The bar indicates 100 nm.

recA) and temperature (37°C) have to be sufficiently high; these conditions were determined to yield saturation length at the titration point (see Materials and methods and DiCapua *et al.*, 1990). Because negatively stained specimens of unfixed recA–ssDNA complexes contained two structures, one with the parameters and contour length of the complexes in amorphous ice and another with the parameters and contour length of the fixed and stained complexes but more variable (DiCapua *et al.*, 1990; Table I), as well as hybrid circles with patches of both structures and intermediate contour length, the experiments on the binding stoichiometry were performed with fixed complexes which always showed a pitch of 64 Å. This means that all measured values presented would need to be corrected by a factor of 1.17 (= 75 Å/64 Å) to get the actual values in solution.

Figure 2 shows the contour length of complexes formed on M13 DNA (7240 nt) as a function of the input stoichiometry. The micrographs show selected points of this experiment, one where recA is in excess (3 nt/recA) and where recA self-polymers are visible in the background, one at the titration point (6 nt/recA) where this background has

**Table II.** Pitches of compact recA filaments obtained from electron micrographs of samples in amorphous ice (see Figure 1) or after fixation with glutaraldehyde and negative staining with uranyl acetate

Sample	Amorphous ice		Fixed and stained	
	Pitch (Å) <sup>a</sup>	<i>n</i>	Pitch (Å) <sup>b</sup>	<i>n</i>
Self-polymer	76 ± 2	30	63 ± 1	8
Self-polymer + 1 mM ATP <sub>γ</sub> S	78 ± 3	35	62 ± 3	15
Complex of recA with 6 nt/recA of ssDNA	76 ± 2	38	64 ± 2	19

<sup>a</sup>By measuring the length of 10 helical turns.<sup>b</sup>Measured by optical diffraction of low dose electron micrographs.

largely disappeared, and the last where DNA is in excess (12 nt/recA), where the contour length of the complexes is clearly shorter, indicating that all the DNA molecules have bound recA, but that each has less recA bound to it. The local structure of these three examples is indistinguishable: they have the same width and same axial repeat of 64 Å, as measured by optical diffraction on low dose EM negatives [insets, Figure 2; at 6 nt/recA  $64 \pm 2$  Å ( $n = 19$ ), at 9 nt/recA  $64 \pm 2$  Å ( $n = 17$ ), and at 12 nt/recA  $65 \pm 3$  Å ( $n = 8$ )]. It is surprising that the complex at DNA excess has an uninterrupted appearance; for a well structured interaction, one would expect instead to see patches of binding separated by unbound DNA. In contrast, the regularity of the recA coat suggests that any number of nucleotides above six per recA can be incorporated into the complex. Alternatively, loops of uncomplexed DNA may be located at the few visible kinks observed in complexes with excess DNA (ss DNA collapses into tight structures not easily seen by EM). Kinks, however, are always found when the radius of curvature becomes too small to accommodate the stiffness of the complex. It is surprising in any case that the recA distributes evenly between all the DNA molecules. This distribution was investigated further by taking a recA–DNA mixture at 6 nt/recA [with a contour length of  $1.95 \pm 0.06$  Å/nt ( $n = 14$ )] and adding an additional amount of 6 nt/recA of DNA. After 30 min further incubation, a homogeneous population was observed with a contour length of  $1.04 \pm 0.1$  Å/nt ( $n = 31$ ), the same as a sample made directly at an initial stoichiometry of 12 nt/recA [ $1.05 \pm 0.06$  Å/nt ( $n = 18$ )], indicating full and equal redistribution of recA. The redistribution was ~80% complete after 10 min, while after 1 min, it was only beginning, as reflected by a mixture of very short kinked complexes ( $<0.5$  Å/nt) and circles that still had the original length. At these shorter time points, we did not find discrete size classes which might be expected if secondary structure elements were removed from the DNA in sequential steps (due to the relative sequence-dependent stability of the DNA duplex stretches) during the redistribution. However, our data set was too small to exclude this mechanism.

The contour length of complexes was plotted as a function of input stoichiometry in Figure 2d (the actual values from one particular experiment are shown as an inset to illustrate the contour length distribution). We can see that the contour length is at a plateau at input stoichiometries above one recA per 6 nt and then decreases when more DNA is present. The data points are seen to follow the theoretical curve calculated for full binding of all the recA up to saturation of one recA per 6 nt: accordingly, at 12 nt/recA input, the complexes are half as long as at 6 nt/recA, at 18 nt/recA input, one-third as long, as predicted if all the recA would (i) distribute evenly to all the DNA molecules and (ii) form the same

structure. If saturation were at 5 nt/recA, the stippled line would have resulted, with half length at 10 nt/recA. While the results from many independent experiments fit the curve for one recA unit per six nucleotides, a saturation at 7 or 5 nt/recA cannot be excluded, because the concentrations of both recA and DNA need to be known to within an error of  $<10\%$ . The recA protein concentration may be wrong by up to 10–20%, since it is not highly purified (we routinely omitted columns after the first step in the purification procedure because, although they improved the appearance on the protein gel slightly, they tended to reduce the specific activity—perhaps due to inactivation of some of the protein). If pure, active, recA makes up  $<100\%$  of our protein concentration (assuming that the latter includes some impurities), then the actual input stoichiometry would be more nt/recA, shifting the abscissa of Figure 2d to the left, resulting in an apparent titration point at 7 nt/recA rather than 6. On the other hand, using an extinction coefficient of 5.9 (Craig and Roberts, 1980) rather than 6.33 (Tsang *et al.*, 1985) would lead to an increase of the measured concentration by 7%, this time leading to fewer nt/recA, i.e. an apparent titration point at 5.5 nt/recA. Analogously, using an extinction coefficient of 8.5 (purely ssDNA) for M13 ssDNA instead of 7.3 would decrease the DNA concentration by 15%, leading to 5.2 nt/recA.

The mass per length of the complex can now be calculated from the two numbers obtained from the plot of Figure 2d, i.e. a length of 2.0 Å per nucleotide and a mass of one recA per 6 nt. If the number obtained is compatible with the values measured by independent methods, then we will have demonstrated the stoichiometry from a third point of view. The length per nucleotide should first be corrected for the shrinkage induced during EM preparation by the factor mentioned above, 1.17; the result, 2.3 Å/nt, multiplied by 6 nt/recA, yields 13.8 Å/recA. This corresponds to a mass per length of 7.25 recA per 100 Å.

#### The mass per length of the compact form

Independent estimates of the mass per length have been obtained by small angle neutron scattering, by STEM, by image reconstruction (Yu and Egelman, 1992) and by crystallography (Story *et al.*, 1992).

In small angle neutron scattering, the number of scattered neutrons is proportional to the mass of matter in the solution. In order to calculate the mass per molecule, one then needs first to subtract the intensity of scattering due to the mass of solvent (a relatively large number) and then to divide the remaining value by the number of particles, i.e. the concentration (an experimental value with its own error, as discussed above). Therefore, the absolute value of the mass per length does not follow directly from the measurement. However, when neutron scattering experiments are done on

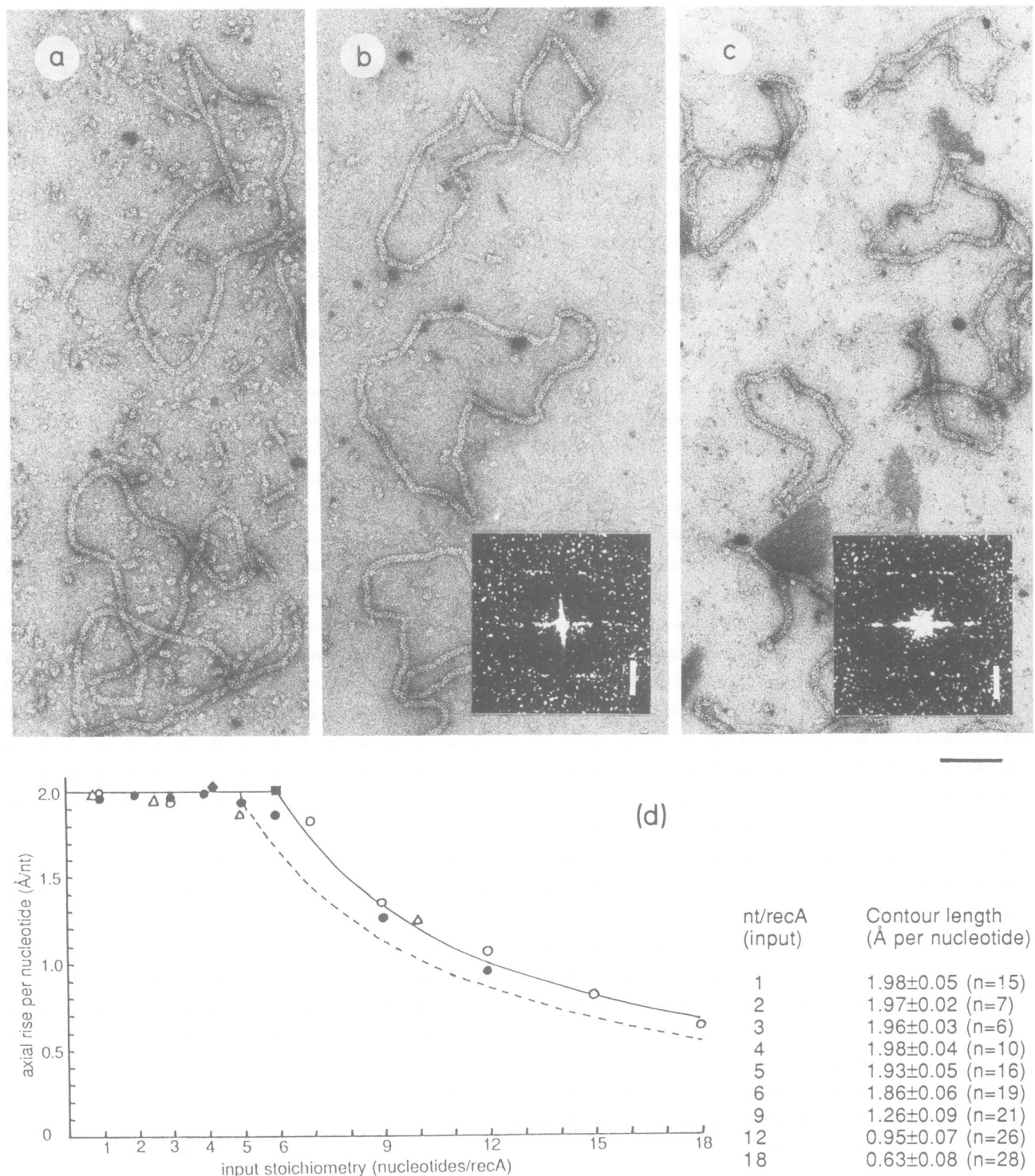


**Fig. 2.** Contour length of compact ssDNA complexes as a function of input stoichiometry. (a, b and c) Examples of electron micrographs used for the contour length measurements, at input stoichiometries of 3, 6 and 12 nt/recA. Samples were fixed and prepared for EM by negative stain. The bar indicates 100 nm. The insets show optical diffraction from the same samples photographed at low electron dose. The bar indicates 0.01 Å<sup>-1</sup>. (d) Contour length (normalized to Å/nt) of complexes as a function of input stoichiometry. The various symbols stand for independent series of experiments performed in part (open and filled circles) at an interval of 2 years with different recA and DNA preparations. The actual data from experiment (●) are shown at the side to indicate the standard deviations of the measurements. The full line is the theoretical curve assuming 'stoichiometric' binding of one recA per 6 nt, and the dashed line for one recA/5 nt.

ssDNA complexes in the absence (compact) or presence (open) of ATP $\gamma$ S, on the same day with the same preparation and under the same conditions, one may retain the ratio of the  $I_0$  (intensity at zero scattering angle; the mass per length follows from  $I_0$ /concentration) of the compact and the open

complexes since the protein concentration and the contrast factors are divided out. In such experiments we observed a ratio of the mass per lengths of  $1.16 \pm 0.04$  (six experiments). Starting from the well established mass/length for the open complex of 6.4 recA per 100 Å (6.17 recA

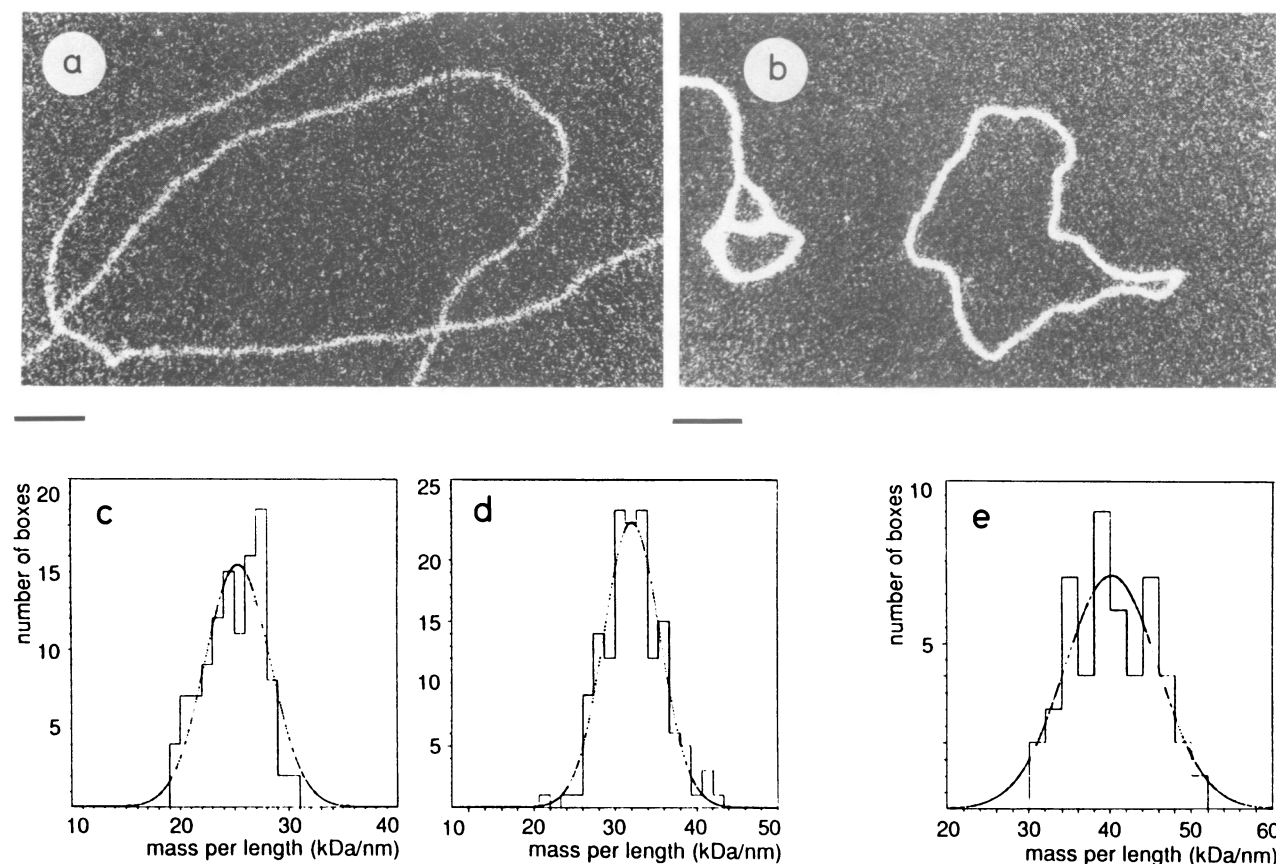


**Fig. 3.** Mass per length determination by STEM. Dark field images of the open (a, in the presence of ATP $\gamma$ S) and the compact (b) complex of recA with ssM13 DNA at 6 nt/recA, fixed with glutaraldehyde. The bars indicate 100 nm. The histograms show the mass per length analysis of unfixed open complexes (c), fixed open complexes (d) and fixed compact complexes (e).

**Table III.** Measurement of mass per length of recA–ssDNA complexes by STEM

Sample	mass/length (kDa/100 Å)	Interpretation
Open complex (ATP $\gamma$ S)		
Unfixed	$245 \pm 24$ (100 segments)	$6.2 \pm 0.6$ recA/100 Å gain of 31% mass
Fixed	$322 \pm 22$ (100 segments)	
Compact complex		
Fixed (exp. 1)	$403 \pm 56$ (50 segments)	correction for 31% glutaraldehyde leads to $307 \pm 43$ kDa/100 Å i.e. $7.7 \pm 1.0$ recA/100 Å $334 \pm 19$ kDa/100 Å i.e. $8.3 \pm 0.3$ recA/100 Å
(exp. 2)	$439 \pm 25$ (50 segments)	

Note that in this table we did not correct for the change from 75 Å to 64 Å pitch usually caused by fixation and adsorption.

per turn of 95 Å pitch), this would imply a mass/length for the compact complex of  $7.4 \pm 0.3$  recA/100 Å.

The mass per length of compact complexes was measured by STEM by analysing the elastically scattered electrons collected on an annular detector. We wish to discuss a weakness of this determination, which lies not with the method, but with the sample: compact complexes are not stable structures, but rather, snapshots of a dynamic equilibrium of binding. The protein redistributes quickly between the available DNA and the contour length decreases upon lowering the temperature or upon dilution. Therefore, recA tends to fall off during the adsorption and washing procedure necessary for the STEM sample preparation.

Indeed, when we tried washing an adsorbed sample of unfixed filaments to remove salt, we lost the filaments. Yu and Egelman (1992) prepared their samples in a solution of volatile salts for stabilization but did not fix them. They measured  $4181 \pm 366$  daltons/Å, which after correction for the adsorption/dehydration shrinkage described above, would correspond to  $9 \pm 0.8$  recA units per 100 Å (a recA unit is approximated to 40 kDa, including about six nucleotides).

We decided to fix our sample with glutaraldehyde and then wash extensively after adsorption on carbon film to remove all salt. Glutaraldehyde attaches to the amino groups of the protein, thereby adding mass to the particles. This increase in mass was 'scaled' on a reference sample, the ATP $\gamma$ S-



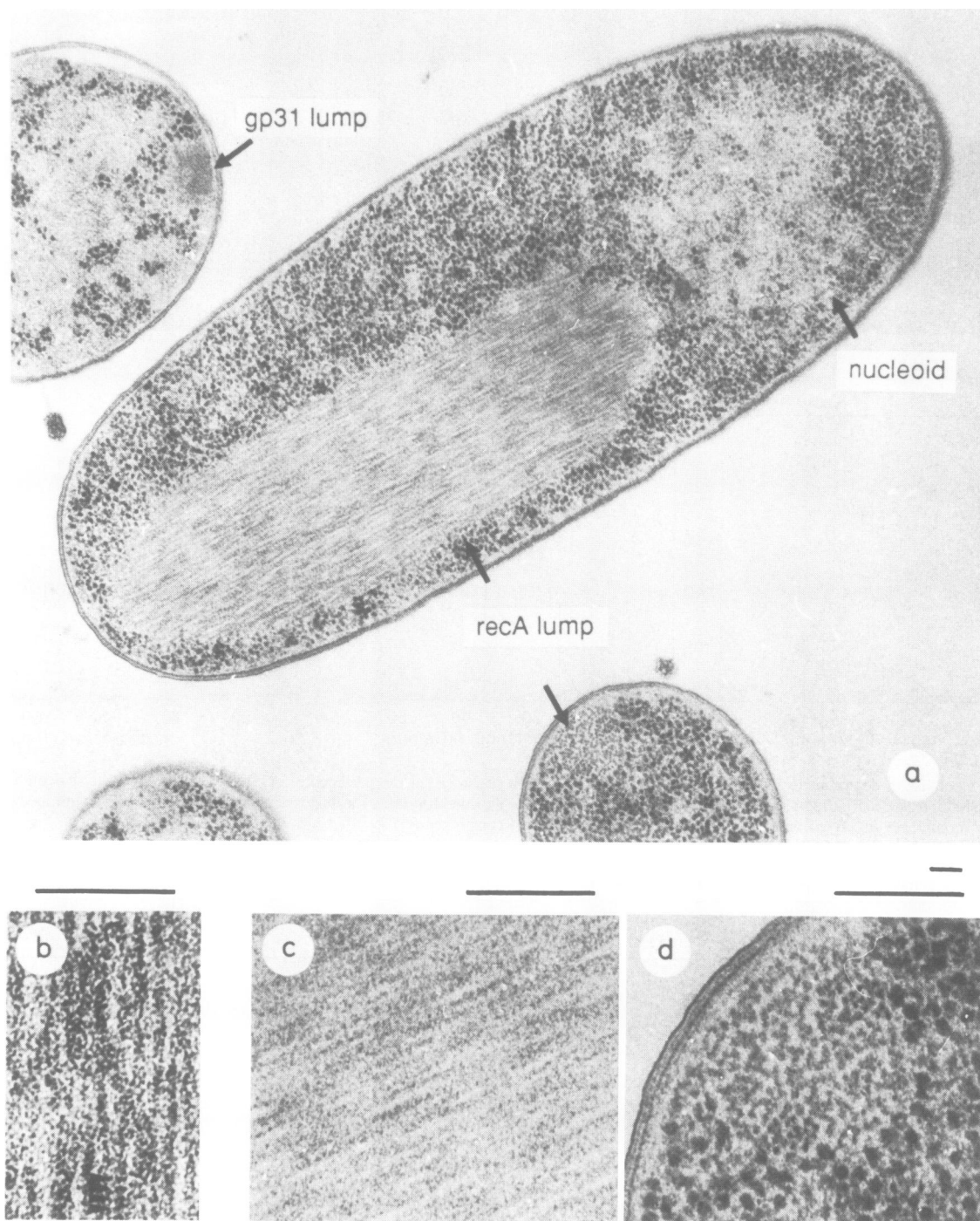


**Fig. 4.** Thin sections of bacterial cells overproducing recA. **a**, **c**, and **d** are embedded in Epon, **b** in Lowicryl HM20. The bars indicate 100 nm. As a comparison for non-fibrous inclusion bodies, *E. coli* cells overproducing the T4 phage gp31 protein were mixed into the recA cells (top left).

stabilized complex with ssDNA. This filament yielded the same mass per length as the ATP $\gamma$ S-stabilized complex with dsDNA, 6.4 recA/100 Å (Figure 3 and Table III), a value well established also by image reconstruction (Yu and Egelman, 1990) for the open form of the recA filament. After fixation, we reproducibly observed an increase of mass in the order of 31% (Table III) between the unfixed sample and the sample fixed with glutaraldehyde (fixed under the same conditions as the compact complex). The use of this factor for correction of another sample with another structure introduces a considerable uncertainty. The experiment with

the fixed compact structure was performed twice (Table III); after correction for the mass addition by glutaraldehyde and a shrinkage from 75 Å pitch to 64 Å, one obtains values of  $6.6 \pm 1.0$  and  $7.1 \pm 0.3$  recA/100 Å.

We see that the mass per length of 7.25 recA per 100 Å derived in the preceding section from the measured axial rise per nucleotide and the stoichiometry, lies close to the independent estimates from neutron scattering and STEM, which gives support to the hypothesis of six nucleotides per recA for the stoichiometry of binding. Fourier analysis of selected electron micrographs of frozen hydrated specimens

has yielded six units per turn of 78 Å (Yu and Egelman, 1992), i.e. a mass per length of 7.7 recA/100 Å. The crystal (McKay *et al.*, 1980), contains 6.0 recA per turn of 83 Å pitch, i.e. 7.3 recA per 100 Å.

Yu and Egelman (1992) have calculated a stoichiometry of 5.5 nucleotides per recA (from the axial rise per nucleotide of saturated complexes on electron micrographs, combined with the axial rise per recA subunit obtained by image reconstruction) and they argued that an integer number of 5 nt/recA would be more likely. Our data do not exclude 5 nt/recA or 7 nt/recA. The important result from both studies is that the data agree to exclude the stoichiometry of three nucleotides per recA which had been postulated previously, leading to the important conclusion that the two complexes of recA with ssDNA, the one in the absence of ATP at ~6 nt/recA, and the one in the presence of ATP at 3 nt/recA, cannot interconvert without a major rearrangement (DiCapua *et al.*, 1990; Yu and Egelman, 1992).

### The 75 Å pitch form can be found in the cell

Cells of the recA overproducing strain of *E. coli* (Materials and methods) were grown and induced with nalidixic acid for 60 min. At that time they were prepared for thin sectioning (by rapid freezing and embedding by freeze-substitution). Figure 4 is a micrograph showing sections through bacteria; they reveal inclusion bodies made of the overproduced recA that were cut both longitudinally (whole bacterium of Figure 4) and transversally (bottom right). In the first case we see a lengthwise striation apparently reflecting a parallel array of filaments, and in the other case, a section across an apparently ordered bundle of filaments.

The sideways distance between filaments was found to be ~100 Å both in longitudinal and in cross-section, compatible with the distance to be expected between filaments in the compact form which are ~110 Å in diameter. An interesting question is the nature of the black stain in the axis of the sectioned filaments: it could reflect a water-filled hollow, lined with amino acid side chains that bind uranyl acetate, or a DNA molecule in the axis, as in the compact recA–DNA complexes; as the DNA would make up only 4.5% of the mass of such a complex, it is beyond the possibilities of EM to demonstrate the presence or absence of DNA. Experiments performed by Z-contrast on such samples revealed that the inclusion bodies consist essentially of protein (Haider and Bohrmann, 1990); antibodies to DNA did not bind to the inclusion bodies in the thin sections, even after digestion of the protein with proteases in order to remove screening-off effects [with the same antibody, the nucleoid was heavily labelled (unpublished results and Bohrmann *et al.*, 1990)]. Both methods, however, need concentrations of DNA in the order of mg/ml in order to give a signal.

Closer inspection of the longitudinally cut inclusion bodies reveals a cross-striation along some stretches of the filaments (enlarged detail of Figure 4). The repeat length of this feature was measured with a ruler on enlarged prints for stretches of 3–11 repeats, yielding a value of  $76 \pm 2$  Å (from 16 stretches with a total of 69 repeats). Two micrographs from two different embeddings were used for this analysis (Figure 4) and gave the same results. Although easily seen by eye on single filaments, the repeat did not show up in Fourier transforms of selected areas. In principle, a striation effect

could result from moiré patterns of different layers of filaments, and we cannot rule out this possibility. However, the fact that the longitudinal repeat is the same as the pitch of the compact complex, and that it was found in two independent embeddings, suggests that we are looking at the helices of the compact form of recA. Fibrous structures, with or without longitudinal repeat, were never observed in lumps of other over-expressed proteins (see the gp31 lumps in Figure 4).

This repeat value supports the argument of the compact form being the storage form of recA, therefore with biological significance. Para-crystalline bundles of purified recA *in vitro* have been described that formed at high magnesium or spermidine concentrations (Griffith and Shores, 1985; Williams and Spengler, 1986). Story *et al.* (1992) have argued that 'bundling' of recA may be part of the mechanism to keep recA inactive when not needed, since amino acid mutations that make recA constitutively active are located, in the crystal, at the interface between the helices, and may therefore activate recA by preventing bundling.

### Conclusions

Under conditions where no enzymatic activity can be detected, recA adopts only one structure (which we called compact, 'compressed' in Yu and Egelman, 1992). Using EM of samples in amorphous ice we found a value of 76 Å for the pitch of both the self-polymer and the complex with ssDNA in the absence of nucleotide cofactor, and this both under conditions of excess recA and excess DNA. It is remarkable that the self-polymer and the compact complex with ssDNA have the same pitch and undergo the same shrinkage upon preparation for classical EM by fixation and negative staining.

The local binding stoichiometry of 5–7 nt/recA can be considered as established by the contour length experiment, a value clearly different from the 3 nt/recA postulated in the models for strand exchange.

The simplified model obtained by model-fitting of small angle neutron scattering spectra with five recA units per turn of 70 Å pitch (DiCapua *et al.*, 1990), is not compatible with the data obtained in this paper, namely 76 Å helical pitch by cryo-EM and  $5.6 \pm 0.2$  recA units per turn (from the mass per length relative to the open structure). The solution data will now have to be model-fitted with the more refined model of a non-integer number of subunits per turn, and with the model obtained by image reconstruction (Yu and Egelman, 1992).

Finally, the filaments with 76 Å repeat were found in the cell as well as *in vitro*, indicating that they have a biological reality. It seems likely that recA crystallized (McKay *et al.*, 1980) in a configuration similar to this inactive state (the change in pitch to 83 Å possibly being induced by crystal packing constraints, arising if the recA polymer in solution does not have an integer number of units per turn) rather than in the form it adopts in the active complex with DNA and ATP.

### Materials and methods

#### Materials

For reasons of continuity, all materials were as in DiCapua *et al.* (1990). RecA protein ( $M_r = 37\ 800$ ) was extracted from strain pDR1453/KM4104

according to Weinstock *et al.* (1979) up to the phosphocellulose column chromatography step. The concentration was determined by absorbance using  $E_{1\%, 270\text{ nm}} = 6.33$ . Single-stranded DNA was from phage M13 mp19. The concentration of M13 ssDNA was determined by absorbance using  $E_{1\text{ mm}, 260\text{ nm}} = 7.3$ .

### Samples

Complexes and self-polymers of recA protein were prepared by incubation of the protein (and DNA where occurring) at a protein concentration of  $\sim 25\text{ }\mu\text{M}$  (1 mg/ml) for conventional EM, 50–100  $\mu\text{M}$  (2–4 mg/ml) for cryo-EM, in the presence of 2 mM  $\text{Mg}(\text{acetate})_2$  for 30 min at the temperature of the assay, i.e.  $37^\circ\text{C}$ , except for the experiments where the temperature was varied. The buffer was 20 mM potassium phosphate (50:50  $\text{K}_2\text{HPO}_4$  and  $\text{KH}_2\text{PO}_4$ , pH  $\sim 6.9$ ) and contained between 1 and 4% glycerol (due to the addition of recA from a stock 10 mg/ml in 10% glycerol storage buffer).

For the contour length experiments on complexes with ssDNA, control experiments were performed to assess full binding. (i) The contour length depends strongly on temperature of incubation up to  $\sim 30^\circ\text{C}$ , while at  $37^\circ\text{C}$  essentially saturation length is found (DiCapua *et al.*, 1990). (ii) The contour length decreases at low concentrations of a constant DNA/recA mixture: at 1  $\mu\text{M}$  recA, only 70% of saturation length is found, while between 20 and 100  $\mu\text{M}$  recA we saw no more increase. (iii) Buffer conditions:  $\text{Mg}(\text{acetate})_2$  concentration (between 0 and 10 mM) had no effect; Tris pH 7.6 gave the same result as potassium phosphate pH 6.9. (iv) DNA sequence and secondary structure: there was no difference in contour length (normalized to length/nt) between saturated complexes with  $\Phi\text{X174}$  DNA and M13 DNA; boiling of the DNA to remove secondary structure just before complex formation also had no effect on length. Complexes with etheno-derivatized M13 DNA (which cannot form secondary structure) also had the same contour length.

### Methods

**Conventional EM.** This was done as in DiCapua *et al.* (1990). Samples were fixed with 0.1% glutaraldehyde (a fresh dilution in 100 mM phosphate buffer), diluted to 50  $\mu\text{g}/\text{ml}$  protein, adsorbed onto the clean face of a carbon film on mica, stained with uranyl acetate (1% in water) and air-dried. Negatively stained catalase crystals were used for calibration of the magnification (Wrigley, 1968). Pitches derived from negatively stained specimens were measured by optical diffraction (also calibrated with images of the catalase crystal) on micrographs taken at low electron dose.

**EM in amorphous ice.** This was done as in Hewat *et al.* (1991) essentially by the standard procedure of Dubochet *et al.* (1985). Pitch values were determined by measuring the length of stretches of 10 turns, between the tips of the zigzag, on digitized images. The length of 10 turns was measured on both sides of the filament and the two values obtained were averaged. Only relatively straight segments with each of the turns clearly visible were measured and in cases of slight curvature the curve was approximated by up to three straight segments. This type of measurement gives the average pitch for well preserved filaments and can only be employed when all turns are visible. The EM magnification was calibrated by using the 40 Å first layer line in computed Fourier transforms of microtubule images (Amos and Klug, 1974).

**Mass per length analysis by STEM.** This was performed as described by Müller *et al.* (1992). Samples were adsorbed onto thin carbon films supported by a holey grid, washed by touching briefly on a drop of water four times, and quick-frozen in liquid nitrogen. They were then lyophilized in the electron microscope overnight. The mass per length values were extracted from low dose STEM dark-field images using a software package written for a VAX 3100 workstation.

**Thin section electron micrographs.** *E. coli* KM4104/pDR1453 cells were grown to  $1\text{--}2 \times 10^8$  cells/ml; overexpression of recA was then induced by further incubation with nalidixic acid (40  $\mu\text{g}/\text{ml}$ ) for 60 min. The cells were collected by filtration for 2 min with permanent aeration on a nucleopore filter, and frozen by slamming them on a polished copper block cooled with liquid helium at 6 K (Hobot *et al.*, 1985). Samples were stored in liquid nitrogen until further processing. The samples were substituted for 90 h at 185 K in acetone containing 3% glutaraldehyde in the presence of a molecular sieve (Perform 0.4 nm, Merck) to ensure complete dehydration. The temperature was then raised at a rate of 7.6 K/h to 228 K and kept there for 2 h. Samples were embedded in Lowicryl HM20 at 228 K according to Bohrmann *et al.* (1990). For embedding in Epon, the procedure was the same up to the temperature rise, then as described by Hobot *et al.* (1985). Serial sections (50–60 nm thick) were produced with a LKB

Ultramicrotome III equipped with a diamond knife. They were collected on Formvar/carbon-coated copper grids, and post-stained with uranyl acetate and lead acetate. Micrographs were obtained on a Philips 300 electron microscope operated at 80 kV. The magnification was calibrated using catalase crystals.

### Acknowledgements

We thank Dr Shirley A. Müller for processing the data of Figure 3, Thomas Uetz for preliminary experiments to Figure 4, and Ed Egelman for communication of results prior to publication.

### References

- Amos, L.A. and Klug, A. (1974) *J. Cell Sci.*, **14**, 523–549.
- Bohrmann, B., Arnold-Schultz-Gahmen, B. and Kellenberger, E. (1990) *J. Struct. Biol.*, **104**, 112–119.
- Bryant, F.R., Taylor, A.R. and Lehman, I.R. (1985) *J. Biol. Chem.*, **260**, 1196–1202.
- Cazenave, C., Toulmé, J.-J. and Hélène, C. (1983) *EMBO J.*, **2**, 2247–2251.
- Chang, C.-F., Rankert, D.A., Jeng, T.-W., Morgan, D.G., Schmid, M.F. and Chiu, W. (1988) *J. Ultrastruct. Res.*, **100**, 166–172.
- Craig, N.L. and Roberts, J.W. (1980) *Nature*, **283**, 26–30.
- DiCapua, E., Engel, A., Stasiak, A. and Koller, T. (1982) *J. Mol. Biol.*, **157**, 87–103.
- DiCapua, E., Schnarr, M., Ruigrok, R.W.H., Lindner, P. and Timmins, P.A. (1990) *J. Mol. Biol.*, **214**, 557–570.
- DiCapua, E., Cuillel, M., Hewat, E., Schnarr, M., Timmins, P.A. and Ruigrok, R.W.H. (1992) *J. Mol. Biol.*, **226**, 707–719.
- Dubochet, J., Adrian, M., Lepault, J. and McDowell, A.W. (1985) *Trends Biochem. Sci.*, **6**, 143–146.
- Egelman, E.H. and Stasiak, A. (1986) *J. Mol. Biol.*, **191**, 677–697.
- Flory, J., Tsang, S.S. and Muniyappa, K. (1984) *Proc. Natl. Acad. Sci. USA*, **81**, 7026–7030.
- Griffith, J. and Shores, C.G. (1985) *Biochemistry*, **24**, 158–162.
- Haider, M. and Bohrmann, B. (1990) *Proceedings of the XIIth International Congress for Electron Microscopy*. San Francisco Press, pp. 186–187.
- Heuser, J.E. and Griffith, J. (1989) *J. Mol. Biol.*, **210**, 473–484.
- Hewat, E.A., Ruigrok, R.W.H. and DiCapua, E. (1991) *EMBO J.*, **10**, 2695–2698.
- Hobot, J.A., Villiger, W., Escaig, J., Maeder, M., Ryter, A. and Kellenberger, E. (1985) *J. Bacteriol.*, **162**, 960–971.
- Koller, T., DiCapua, E. and Stasiak, A. (1983) In Cozzarelli, N.R. (ed.), *Mechanisms of DNA Replication and Recombination*. Alan Liss, New York, pp. 723–729.
- Kowalczykowski, S.C. (1991) *Annu. Rev. Biophys. Chem.*, **20**, 539–575.
- Little, J.W. and Mount, D.W. (1982) *Cell*, **29**, 11–22.
- Mckay, D.B., Steitz, T.A., Weber, I.T., West, S.C. and Howard-Flanders, P. (1980) *J. Biol. Chem.*, **255**, 6662.
- Menetsky, J.P. and Kowalczykowski, S.C. (1985) *J. Mol. Biol.*, **181**, 281–295.
- Müller, S.A., Goldie, K.N., Bürki, R., Häring, R. and Engel, A. (1992) *Ultramicroscopy*, in press.
- Roca, A.I. and Cox, M.M. (1990) *CRC Crit. Rev. Biochem. Mol. Biol.*, **25**, 415–455.
- Silver, M.S. and Fersht, A.R. (1982) *Biochemistry*, **21**, 6066–6072.
- Slilaty, N.S. and Little, J.W. (1987) *Proc. Natl. Acad. Sci. USA*, **84**, 3987–3991.
- Stasiak, A. and Egelman, E.H. (1986) *Biophys. J.*, **49**, 5–6.
- Story, R.M., Weber, I.T. and Steitz, T.A. (1992) *Nature*, **355**, 318–325.
- Takahashi, M. and Schnarr, M. (1989) *Eur. J. Biochem.*, **183**, 617–622.
- Takahashi, M., Kubista, M. and Norden, B. (1989) *J. Mol. Biol.*, **205**, 137–147.
- Timmins, P.A., Ruigrok, R.W.H. and DiCapua, E. (1991) *Biochimie*, **73**, 227–230.
- Tsang, S.S., Chow, S.A. and Radding, C.M. (1985) *Biochemistry*, **24**, 3226–3232.
- Williams, R.C. and Spengler, S.J. (1986) *J. Mol. Biol.*, **187**, 109–118.
- Weinstock, G.M., McEntee, K. and Lehman, I.R. (1979) *Proc. Natl. Acad. Sci. USA*, **76**, 1638–1642.
- Wrigley, N.G. (1968) *J. Ultrastruct. Res.*, **24**, 454–464.
- Yu, X. and Egelman, E.H. (1990) *Biophys. J.*, **57**, 555–566.
- Yu, X. and Egelman, E.H. (1992) *J. Mol. Biol.*, **227**, 334–346.

Received on July 20, 1992; revised on September 8, 1992